JOURNAL OF CATALYSIS 101, 201–211 (1986)

On the Role of Specific Hydrogen Adsorption Sites in Methanol Decomposition on Zinc Oxide

D. L. ROBERTS AND G. L. GRIFFIN

Department of Chemical Engineering and Materials Science, University of Minnesota, Minneapolis, Minnesota 55455

Received December 17, 1985; revised April 18, 1986

We have combined temperature-programmed desorption, infrared spectroscopy, and selective site blocking experiments to determine the importance of Type I H_2 adsorption sites for the decomposition of CH_3OH on ZnO catalysts. Methanol adsorbs dissociatively at both Type I and non-Type I cation–anion pair sites. Methoxy groups formed at Type I sites decompose at slightly lower temperature than $CH_3O_{(a)}$ groups at non-Type I sites. The apparent activation energies for this step are 31 ± 1 and 33 ± 1 kcal/mol at the Type I and non-Type I sites, respectively. At both sites, $CH_3O_{(a)}$ decomposition leads to H_2 desorption and formation of adsorbed $HCOO_{(a)}$ species. These species decompose at the same temperature on both types of sites, with an apparent activation energy of 40 ± 1 kcal/mol. However, the ratio of $CO:CO_2$ during $HCOO_{(a)}$ decomposition is larger on the Type I sites. The Type I sites can be blocked throughout the CH_3OH adsorption and decomposition cycle by preadsorption of H_2O. This H_2O is dissociatively adsorbed, with a unique OH stretching frequency at 3672 cm^{-1} and an adsorption energy of 40 ± 3 kcal/mol. These results are interpreted to suggest that Type I sites on ZnO probably do *not* have a major role in the CH_3OH synthesis reaction on Cu/ZnO catalysts.

INTRODUCTION

Zinc oxide is well known as a major component of commercial Cu/ZnO methanol synthesis catalysts. Although it is the addition of copper to zinc oxide that is responsible for greatly enhancing the rate of methanol synthesis in these catalysts, the role of the ZnO phase remains the subject of debate (*1–13*). Several authors (*14–23*), ourselves included, have proposed that the H_2 adsorption step required for CO hydrogenation activity takes place on the Type I H_2 adsorption sites on the ZnO phase. These sites accomplish the heterolytic dissociation of H_2 at room temperature to produce infrared active Zn—H and O—H surface species. Attempts to prove the importance of Type I sites are complicated, however, by the fact that several other adsorption states for H_2 exist on ZnO (*24–29*). Indeed, to our knowledge the only demonstration of a direct connection between Type I H_2 adsorption behavior and hydrogenation activity was provided by Dent and Kokes (*25*), who demonstrated that Type I sites participated in the hydrogenation of ethylene.

Type I sites are known to be generated by high-temperature treatment of ZnO (ca. 673 K, in either vacuum, H_2, or O_2 environments (*26*)). Neither the concentration of the sites nor the vibrational frequency of $H_{(a)}$ species adsorbed at the sites are affected by exposure to O_2, a pretreatment step which is frequently used in adsorption studies to improve the IR transmission characteristics of the bulk ZnO powder. Thus the Type I sites appear *not* to be associated with O^{2-} anion vacancies. Several additional IR and/or TPD studies have shown that CO_2 (*21, 30*) and H_2O (*20, 25, 26*) adsorb competitively with Type I H_2, whereas CO adsorbs noncompetitively (*15, 18, 22, 23, 26*). However, studies are lacking which clearly resolve the interaction between the Type I sites and species such as CH_3OH, HCOOH, and H_2CO during adsorption and decomposition on ZnO or Cu/ZnO mixtures.

We therefore decided to perform a care-

0021-9517/86 $3.00

ful study of the adsorption and decomposition of CH_3OH on ZnO surfaces containing known concentrations of Type I sites, in order to examine the possible role of Type I sites in the methanol synthesis reaction on ZnO-based catalysts. Additional information has also been obtained by "selective poisoning" experiments (*31*), in which the Type I sites are initially blocked with a second coadsorbed species such as H_2O. Finally, these experiments provide additional information about the geometry and properties of the Type I sites themselves.

EXPERIMENTAL

Combined infrared and temperature-programmed desorption (TPD) experiments were performed using our previously described vacuum cell (*32*). A 50-mg sample of ZnO powder (Kadox 25, Gulf Western Natural Resources, BET surface area = 10 m^2/gm) was deposited from an aqueous slurry onto the front face of the cell mirror. Infrared spectra were obtained in a transmission-reflection mode at a rate of 1–2 scans/sec (total scans = 800) at a resolution of either 4 or 8 cm^{-1}, using a Nicolet 60-SX FT-IR spectrometer equipped with an MCT detector. During the TPD warmup (heating rate = 0.4 K/sec), IR spectra were taken at regular temperature intervals (75 scans/spectrum), while desorbing species were monitored with a quadrupole mass spectrometer (Spectramass 800) scanning over the range m/e = 1 to 50.

A typical pretreatment to activate the Type I H_2 sites involved (step 1) heating the sample under vacuum ($P < 10^{-6}$ Torr) at 673 K for 3 h (step 2) cooling to 573 K and admitting 0.5 Torr O_2 for 10 min, then evacuating (O_2 dosing repeated three times), (step 3) rewarming under vacuum to 673 K for 20 min before cooling to 300 K. Measured amounts of CH_3OH and/or H_2O were then admitted to the sample at room temperature.

The adsorption procedure for H_2 TPD experiments consisted of exposing the sample to 40 Torr H_2 for 10 min at 300 K, followed by cooling to 100 K and then evacuating. The amount of Type I H_2 adsorbed on the sample was then determined by integrating the area under the H_2 TPD spectrum and multiplying by the spectrometer calibration factor for H_2. In addition, since the infrared intensity of the Zn—H band in the presence of 40 Torr H_2 was not significantly different at 300 K than at 100 K, this procedure also confirmed that the Type I H_2 coverage was close to saturation at 300 K.

RESULTS

The results from the temperature-programmed desorption or decomposition of the pure components H_2O and CH_3OH will be presented first. These will be followed by the results from the TPD experiments using CH_3OH adsorbed on ZnO samples whose Type I sites have been blocked by preadsorbed H_2O.

H_2O adsorption. The IR spectra which demonstrate the competitive adsorption between H_2 and H_2O for Type I sites on ZnO are shown in Fig. 1. The spectra have been displaced vertically for clarity.

The bottom curve shows the IR spectrum in the presence of 40 Torr H_2 over a freshly activated sample at 300 K, prior to adsorbing H_2O. The sharp band at 1709 cm^{-1} and the less intense band at 3491 cm^{-1} correspond to the Zn—H and O—H stretching vibrations, respectively, which are characteristic of H_2 adsorbed on Type I sites (*24*). These bands disappear upon evacuating the H_2, confirming that Type I H_2 adsorption is reversible at room temperature (*25*). We note that the band observed at 3618 cm^{-1} is attributed to a residual surface OH species and is *not* associated with Type I H_2 adsorption. Features in the 2900- to 2800-cm^{-1} region are due to a residual surface hydrocarbon impurity. The concentration of Type I sites for this sample is 5.8 μmol/gm, as determined from an H_2 TPD experiment.

The middle curve in Fig. 1 shows the IR spectrum of the ZnO at 300 K obtained after evacuating the cell to empty the Type I sites, adding H_2O until the Type I sites are

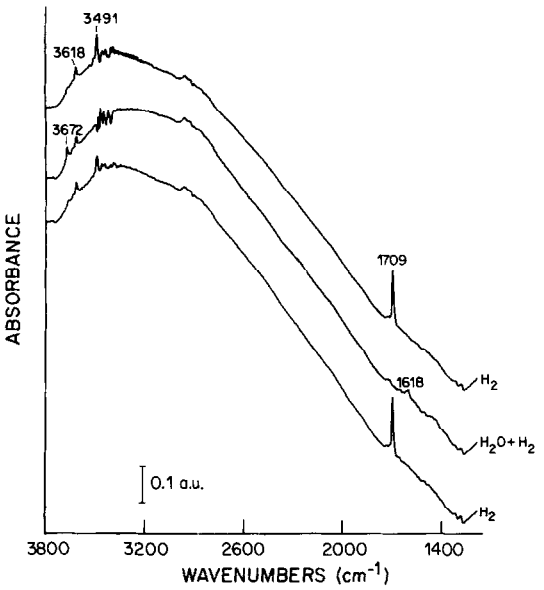

FIG. 1. Infrared spectra of H_2O and H_2 adsorbed on Type I activated ZnO (Kadox 25). Bottom: 40 Torr H_2 alone at 300 K. Middle: 400 Torr H_2 at 300 K, following preexposure to H_2O. Top: 40 Torr H_2 at 300 K for same sample, after heating to 673 K.

completely blocked, and then readmitting 400 Torr H_2. The IR spectrum shows that the bands at 3491 and 1709 cm^{-1} are absent, indicating that the Type I sites are now blocked by irreversibly adsorbed H_2O. In addition, new bands at 3672 and 1618 cm^{-1} have appeared. The band at 3672 cm^{-1} has previously been assigned to an OH species adsorbed onto one of the polar faces of ZnO (*33*), without knowledge that it may have been associated with blocked Type I sites. The earlier band at 3618 cm^{-1} due to residual hydroxyl species has remained essentially unchanged.

Evacuating the 400 Torr H_2 and then warming the sample to 390 K (not shown) causes the band at 1618 cm^{-1} to disappear, while leaving the band at 3672 cm^{-1} unaffected. Therefore, the weak band at 1618 cm^{-1} can be assigned to the H—O—H bending mode of molecularly adsorbed H_2O (*33*).

Continued warming to 673 K causes the band at 3672 cm^{-1} to be removed (not shown). The top curve shows the IR spectrum of the sample obtained after then cooling the sample back to 300 K, adding 0.01 Torr O_2 to improve the IR transmission, and finally readmitting 40 Torr H_2. The bands at 3491 and 1709 cm^{-1} have been completely restored, which confirms that the Type I sites have been reactivated by heating to 673 K. Thus, the H_2O adsorption state which blocks the Type I sites desorbs below 673 K, and is further characterized by a unique $OH_{(a)}$ vibrational band at 3672 cm^{-1}.

The TPD spectrum of H_2O recorded during the warmup of the Type I blocked sample is shown in Fig. 2. The small H_2O desorption shoulder near 390 K corresponds to desorption of the molecular H_2O state producing the weak band at 1618 cm^{-1}. The principal feature is a strongly bound state with a desorption maximum at 599 K. Comparison with the IR spectra recorded during the warm-up confirms that this dissociatively adsorbed H_2O state produces the O—H band at 3672 cm^{-1}, and is the H_2O adsorption state responsible for blocking the Type I H_2 sites.

The adsorption energy for Type I H_2O is 40 ± 3 kcal/mol, based on the TPD equation for porous samples, which allows for diffusion and readsorption of the desorbing species within the catalyst pores (*34*).

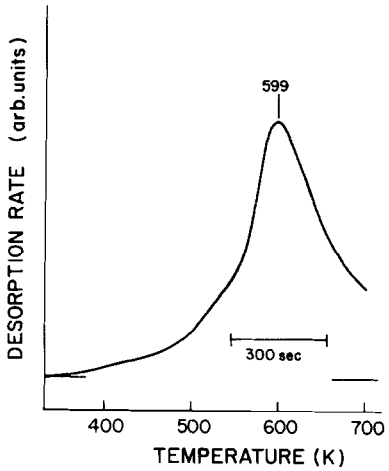

FIG. 2. Temperature-programmed desorption spectrum of H_2O adsorbed in Type I sites on ZnO.

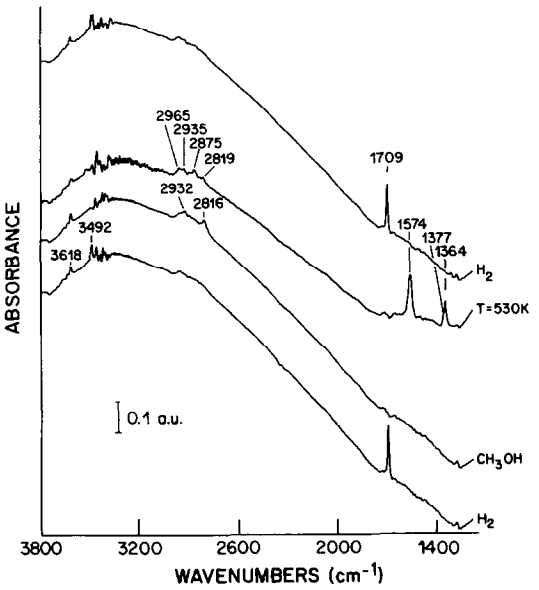

FIG. 3. Infrared spectra of CH_3OH and H_2 adsorbed on Type I activated ZnO (Kadox 25). Bottom: 40 Torr H_2 alone at 300 K. Second: same sample, exposed to CH_3OH. Third: same sample after warming to 530 K. Top: same sample after warming to 673 K, then exposed to 40 Torr H_2 at 300 K.

CH_3OH decomposition. In Fig. 3 we show the IR spectra acquired during the adsorption and subsequent TPD of CH_3OH on Type I-activated ZnO. The bottom curve is the spectrum of the sample under 40 Torr H_2 at 300 K obtained prior to adsorbing CH_3OH. The bands at 3492 and 1709 cm^{-1} confirm the presence of active Type I sites, and the band at 3618 cm^{-1} assigned to residual OH is also present.

The next curve in Fig. 3 is the spectrum obtained after evacuating the H_2 and adsorbing an amount of CH_3OH corresponding to 10 μmol/g at 300 K. The bands appearing at 2932 and 2816 cm^{-1} have been assigned to the asymmetric and symmetric C—H stretching vibrations of the surface methoxy species (*34*). It is interesting to note that the adsorption of CH_3OH produces no new IR-resolvable surface hydroxyl features, nor does it perturb the residual surface hydroxyl band at 3618 cm^{-1}.

The next curve in Fig. 3 is the spectrum of the sample obtained at 530 K during the temperature-programmed decomposition of the adsorbed CH_3OH. The intensity of the methoxy C—H bands at 2932 and 2816 cm^{-1} decreases, and bands appear at 2875, 1574, and 1364 cm^{-1}, with a small shoulder being resolved at 1377 cm^{-1}. These peaks are assigned to the C—H stretching mode, asymmetric and symmetric O—C—O stretching vibrations, and the in-plane C—H bending mode of the surface formate species, respectively (*34*). The asymmetric O—C—O stretching vibration combined with the in-plane C—H bending mode also produces an additional combination band observed at 2965 cm^{-1} (*17*). Thus these results illustrate the sequential conversion of surface methoxy to surface formate, as has been demonstrated previously (*32, 35*).

The uppermost curve is the spectrum of the sample obtained after completing the TPD experiment, cooling from 673 to 300 K, adding 0.01 Torr O_2 to improve the IR transmission, and then admitting 40 Torr H_2. The bands at 3492 and 1709 cm^{-1} characteristic of the Type I sites have been restored which shows that the $CH_3O_{(a)}$ species have been completely eliminated from the Type I sites.

A separate IR experiment was performed by interrupting the programmed decomposition at approximately 530 K (corresponding to the temperature at which the maximum $HCOO_{(a)}$ coverage is observed during the CH_3OH TPD experiment) and quickly cooling the sample to 300 K. This procedure preserved the surface $HCOO_{(a)}$ coverage. Admitting 40 Torr of H_2 to the cell at this stage failed to produce IR bands at 3490 or 1710 cm^{-1}. This indicates that the $HCOO_{(a)}$ species also block the Type I sites.

We also warmed the sample in 40 Torr of H_2 at this stage, in an effort to hydrogenate the $HCOO_{(a)}$ species back to a methoxy species. No evidence for hydrogenation of the formate was observed under these conditions, up to the temperature at which formate decomposition occurred.

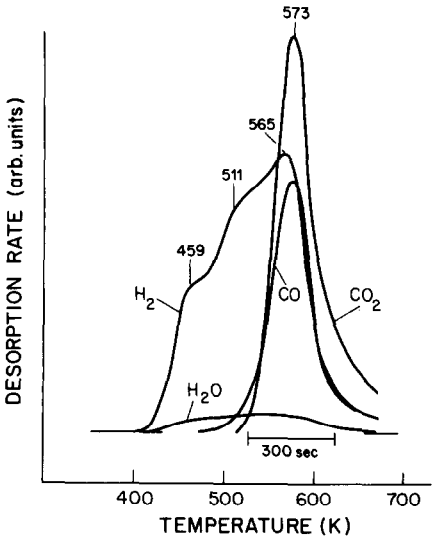

FIG. 4. Product distribution spectra during TPD of CH_3OH adsorbed on Type I activated ZnO (Kadox 25).

The amount of CH_3OH required to completely block the Type I sites is almost twice the number of Type I sites, indicating that CH_3OH also adsorbs at sites other than Type I. The possibility that the excess CH_3OH was adsorbed onto the walls of the system (which did occur in the case of H_2O) can be ruled out, since the rate of CH_3OH adsorption on the walls of the system observed when the sample was saturated was seen to be at least an order of magnitude slower than for H_2O. Furthermore, separate IR experiments showed that CH_3OH does dissociatively adsorb on samples which have been dehydroxylated at a low enough temperature (ca. 523 K) that the Type I sites are not activated.

The product desorption spectra recorded during the acquisition of the IR spectra described in Fig. 3 are shown in Fig. 4. The H_2 evolution curve appears to have three discrete features: a low-temperature shoulder at 459 K, a broader shoulder near 511 K, and a resolvable desorption maximum at 565 K. The H_2 evolution at 565 K is accompanied by the coincident desorption of CO and CO_2 at 573 K. In contrast, the H_2 evolved at 459 and 511 K is not accompanied by any significant amount of carbon oxides. This is a clear indication that the H_2 evolution peaks at 459 and 511 K are a result of the conversion of $CH_3O_{(a)}$ to $HCOO_{(a)}$, while the simultaneous desorption of H_2, CO, and CO_2 at 565–570 K is due to $HCOO_{(a)}$ decomposition. Figure 4 also shows that H_2O is *not* a favored product of either the $CH_3O_{(a)}$ or $HCOO_{(a)}$ decomposition, despite the highly oxidized condition of the ZnO sample.

H_2O + CH_3OH coadsorption. To determine the importance of Type I sites for CH_3OH decomposition, we next performed a series of experiments using preadsorbed H_2O to block the Type I sites before adsorbing CH_3OH. The IR spectra which demonstrate the influence of preadsorbed H_2O on the adsorption of CH_3OH on Type I activated ZnO are shown in Fig. 5. The bottom curve is the spectrum of the sample under 40 Torr H_2 at 300 K obtained prior to adsorbing H_2O. The presence of bands at

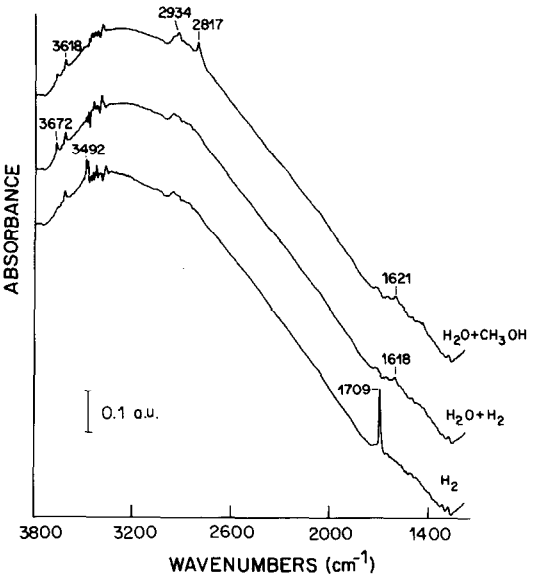

FIG. 5. Infrared spectra of CH_3OH, H_2O, and H_2 adsorbed on Type I activated ZnO (Kadox 25). Bottom: 40 Torr H_2 alone at 300 K. Middle: 40 Torr H_2 at 300 K, following exposure to H_2O. Top: same sample, following evacuation of H_2 and exposure to CH_3OH at 300 K.

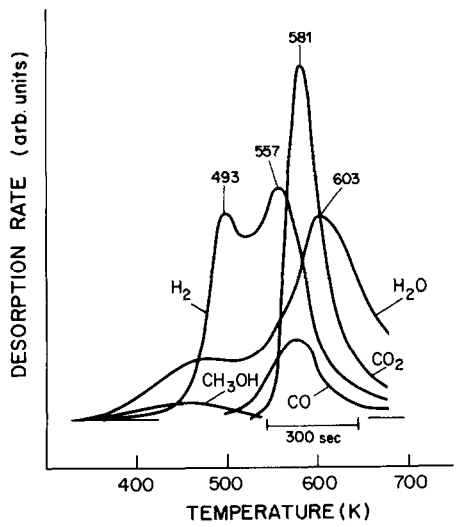

FIG. 6. Product distribution spectra during TPD of coadsorbed CH_3OH and H_2O on ZnO (Kadox 25), where H_2O is blocking Type I sites (cf. Fig. 5).

3492 and 1709 cm^{-1} confirms that Type I sites (5.8 μmol/g) are present initially.

The next curve in Fig. 5 is the spectrum of the sample at 300 K obtained after evacuating the 40 Torr H_2, adsorbing H_2O until the Type I sites were completely blocked, and then readmitting 40 Torr H_2. The absence of bands at 3492 and 1709 cm^{-1} confirms that the Type I sites have been blocked.

The top curve in Fig. 5 is the spectrum of the sample at 300 K obtained after evacuating the 40 Torr H_2 and then adsorbing CH_3OH (10 μmol/g). The $CH_3O_{(a)}$ bands which have grown in at 2934 and 2817 cm^{-1} have almost the same frequency as those previously observed in Fig. 3. The OH stretching vibration at 3672 cm^{-1} has decreased in intensity, suggesting that some of the H_2O adsorbed in Type I sites has been perturbed and/or displaced by CH_3OH. The OH bending mode at 1618 cm^{-1} has changed little in intensity while shifting slightly to 1621 cm^{-1}. The band at 3618 cm^{-1} due to the residual OH species remains essentially unchanged after adsorption of both H_2O and CH_3OH.

The IR spectra acquired during the subsequent programmed decomposition of the CH_3OH adsorbed on the sample whose Type I sites were blocked with preadsorbed H_2O were not significantly different from those obtained earlier during CH_3OH decomposition on ZnO with no preadsorbed H_2O. The only differences were the presence of bands at 3672 and 1618 cm^{-1} due to the preadsorbed H_2O, and the behavior of these was the same as the pure H_2O behavior discussed above.

The TPD product desorption spectra recorded during the preceding experiment are shown in Fig. 6. Except for the appearance of a small H_2O desorption maximum near 475 K in Fig. 6, the H_2O desorption curve is almost identical to the case for adsorbed H_2O alone, with respect to both peak temperature and integrated area (cf. Fig. 2). This leads to two conclusions about the fate of adsorbed H_2O: (1) The molecules adsorbed in Type I sites are not displaced from those sites when the CH_3OH is adsorbed, as might have been inferred from the decrease in intensity of the O—H band at 3672 cm^{-1} (see top curve Fig. 5). Instead, we suggest that the loss of intensity may be due to hydrogen-bonding with neighboring $CH_3O_{(a)}$ species. (2) The preadsorbed H_2O is *not* consumed in the formation of CO_2 during the formate decomposition step. This point is discussed further below.

Figure 6 shows that molecularly adsorbed CH_3OH desorbs between 400 and 500 K. A similar molecular CH_3OH desorption peak could be observed from samples containing no preadsorbed H_2O, if the initial CH_3OH coverage was greater than 10 μmol/g. Thus, there appears to be a finite total concentration of *both* Type I and non-Type I sites at which CH_3OH is dissociatively adsorbed. Addition of CH_3OH beyond this amount is adsorbed into a less tightly bound state which desorbs at 450 K. The low-temperature H_2O desorption state probably involves a similar molecularly adsorbed state.

The dissociatively adsorbed CH_3OH ultimately decomposes to yield H_2, CO, and

CO_2. The H_2 evolution curve shown in Fig. 6 is comprised of two well-resolved maxima at 493 and 557 K; the H_2 desorption shoulder at 459 K that was observed on the H_2O-free surface is absent! The H_2 desorption maximum at 493 K occurs without evolution of any carbon oxides, whereas the maximum at 557 K is accompanied by the evolution of CO and CO_2 with desorption maxima at 576 and 581 K, respectively. Since the sole difference between the experiments shown in Figs. 4 and 6 is the presence of preadsorbed H_2O in the Type I sites, we conclude that *the H_2 peak at 493 K corresponds to the decomposition of surface methoxy species adsorbed at non-Type I sites, while the H_2 desorption feature observed at 459 K can be assigned to the decomposition of methoxy species adsorbed at Type I sites.*

The decomposition of the remaining surface formate species is responsible for the appearance of H_2, CO, and CO_2 between 557 and 581 K. The desorption temperatures are similar to those observed in the absence of preadsorbed H_2O. This indicates that the activation energy of $HCOO_{(a)}$ decomposition is insensitive to Type I vs non-Type I sites.

However, the $CO:CO_2$ product desorption ratio is much smaller now than in the absence of preadsorbed H_2O. As noted above, this is *not* because preadsorbed H_2O at Type I sites is incorporated into the CO_2 product. Instead, it appears that the decrease in CO intensity is correlated with the blockage of Type I sites by preadsorbed H_2O. Thus, we conclude that *Type I sites are selective to CO desorption from the formate intermediate, while non-Type I sites result in the desorption of CO_2.* Thus the presence of adsorbed H_2O affects the $CO:CO_2$ selectivity during CH_3OH decomposition, specifically by affecting the relative concentration of available Type I and non-Type I sites.

It also appears that the H_2 peak at 557 K significantly precedes the CO and CO_2 peaks. This suggests that the delay due to readsorption effects for CO and CO_2 is more pronounced on the samples with preadsorbed H_2O, while diffusion of H_2 out of the sample is unaffected or even slightly facilitated. This delay of CO and CO_2 desorption may result from the formation of transient $CO_{3(a)}^{2-}$ and $HCO_{3(a)}^{-}$ species during diffusion out of the sample.

DISCUSSION

Behavior of Type I sites for methanol decomposition. The IR spectra in Fig. 4 show clearly that CH_3OH adsorbs dissociatively on ZnO. The elimination of the H_2 bands confirms that the Type I sites are blocked. The dissociative nature of the CH_3OH adsorption is confirmed by the frequencies of the asymmetric and symmetric C—H stretching modes for the adsorbed species (ca. 2932 and 2816 cm^{-1}) which differ significantly from the corresponding gas phase values (2977 and 2844 cm^{-1}), and by the fact that only a small amount of molecular CH_3OH desorption is observed during the TPD experiments for initial CH_3OH coverages less than 10 μmol/g. Since the Type I sites have been shown to consist of cation–anion pairs, we can conclude that CH_3OH adsorption produces a methoxy group bound to the surface Zn cation, with a proton transferred to the surface O^{2-} anion:

$$CH_3OH + Zn_{(s)} + O_{(s)} \rightarrow CH_3O—Zn_{(s)} + HO_{(s)} \quad (1)$$

However, it is important to emphasize that reaction (1) is *not* restricted to Type I sites. This is shown by the fact that the number of CH_3OH molecules required to completely block the surface was almost twice the total number of Type I sites in the sample. A similar observation holds for H_2O adsorption, as well. Thus dissociative adsorption of the alcohol OH bond is a general phenomenon that will occur at any unsaturated cation–anion pair site, and is not restricted to those cation–anion pair sites which satisfy the additional criterion of being active for Type I H_2 adsorption.

The next step is the decomposition of the

$CH_3O_{(a)}$ intermediate. Comparison of the results with and without site blocking by H_2O shows several complex differences that may be attributed to the presence or absence of Type I sites. The most obvious difference is the fact that the first H_2 desorption peak occurs 34 K earlier for $CH_3O_{(a)}$ species adsorbed at Type I sites. It is also important to stress the converse of this observation; i.e., that $CH_3O_{(a)}$ species adsorbed in non-Type I sites also decompose readily at temperatures only 34 K greater than for decomposition at Type I sites. Moreover, evolution of H_2 is also observed for decomposition at the non-Type I sites. Since the Type I sites remain blocked until H_2O desorption at 603 K, this indicates that *Type I sites are not essential for either CH_3OH decomposition or H_2 desorption*. Instead, both reactions can occur readily at non Type I sites at elevated temperature.

In contrast to $CH_3O_{(a)}$ decomposition, the decomposition temperature of the $HCOO_{(a)}$ intermediate depends only weakly on whether the species is adsorbed at a Type I or non-Type I site. The H_2 peak observed at 557 K in Fig. 6 associated with $HCOO_{(a)}$ decomposing at non-Type I sites occurs only 8 K earlier than the H_2 peak observed at 565 K in Fig. 4, which contains contributions from $HCOO_{(a)}$ species decomposing at both Type I and non-Type I sites. Similarly, the CO and CO_2 peaks occur at 573 K on surfaces with active Type I sites, and at 576 and 581 K on the surfaces with blocked Type I sites.

The other clear result from Figs. 4 and 6 is the fact that the $HCOO_{(a)}$ decomposition step yields almost exclusively CO_2 on surfaces preexposed to H_2O. This permits us to conclude that CH_3OH molecules adsorbed in non-Type I sites give rise almost exclusively to CO_2 during the $HCOO_{(a)}$ decomposition step. This implies that a neighboring O^{2-} species is available at non-Type I sites that can be incorporated into the formate intermediate and subsequently removed as CO_2. We hope to address the mechanism of replenishment of this O^{2-} anion in a future paper.

The preadsorbed H_2O at Type I sites is *not* incorporated into CO_2, as shown by the fact that H_2O desorption is observed at 603 K, essentially the same temperature as observed after the adsorption of H_2O alone. This indicates that the H_2O molecules which block the Type I sites retain their integrity throughout the CH_3OH decomposition process.

However, it does appear that preadsorbed H_2O causes an increased delay in the diffusion of CO and CO_2 out of the catalyst sample. This delay may result from the transient formation of formate species between CO or CO_2 and $OH_{(a)}$ species adsorbed in Type I sites.

Geometric information about Type I sites. Efforts to identify the geometry of the unique Type I H_2 adsorption sites on ZnO have proceeded steadily since the initial report of their characteristic IR behavior (*24*). The present results add several new pieces of information toward answering this question:

—Adsorbed H_2O molecules in Type I site are significantly more strongly bound than other dissociated H_2O states (i.e., a large H_2O desorption signal is observed during pretreatment of a fresh sample at temperatures up to 623 K, but this temperature is still not high enough to generate Type I sites.

—The adsorbed H_2O in Type I sites has a unique O—H stretching frequency at 3672 cm^{-1}, which is different from the O—H frequency produced by adsorbed H_2 in Type I sites (ca. 3490 cm^{-1}).

—Equally significant is the absence of the 3490-cm^{-1} band when H_2O is adsorbed in Type I sites. That is, the OH group produced at the Type I O^{2-} anion when H_2 is adsorbed has a different vibrational frequency than the OH group produced at the same anion when H_2O is adsorbed.

—The adsorbed CH_3OH state at Type I sites does not produce an OH band in the region above 3500 cm^{-1}.

We have previously presented spectroscopic evidence that Type I sites occur at cation defects on the (0001)-Zn surface (*14*, *15*). The adsorbate geometries expected for H_2, H_2O, and CH_3OH on these sites can be proposed:

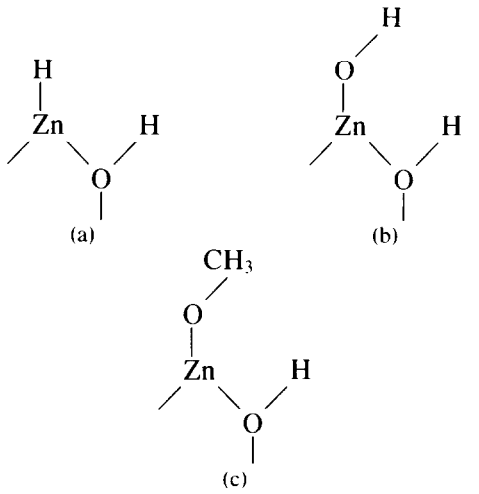

The Type I H_2 infrared peaks at 1710 and 3490 cm^{-1} are assigned to the Zn—H and O—H bonds in structure (a). The latter value for the lattice OH bond is relatively low, which could be accounted for by a minor degree of hydrogen bonding between the $OH_{(a)}$ proton and lone-pair electrons on neighboring O^{2-} anions at the cation vacancy.

The 3672-cm^{-1} peak seen for adsorbed H_2O is assigned to the adsorbed OH group in structure (b). The lattice OH group is not observed at 3490 cm^{-1} as it was for structure (a), probably as a result of the difference in dynamic coupling and/or inductive effects that occur when an $OH^-_{(a)}$ group rather than an $H^-_{(a)}$ ion is present on the neighboring Zn cation. We can speculate that for structure (b), the increased electron withdrawing power of the adsorbed $OH^-_{(a)}$ group removes electron density from the lattice O^{2-} anion, which decreases the O—H stretching frequency of the lattice OH^- group. If the 3490-cm^{-1} band is shifted to lower values, its new value would be masked by the noise in the H-bonding region of our spectra.

Finally, for CH_3OH adsorbed in structure (c), the frequency of the lattice OH^- group will be shifted as for structure (b), and the $CH_3O_{(a)}$ group is present instead of the adsorbed $OH^-_{(a)}$ group. Thus, no isolated OH bands are observed for CH_3OH adsorbed in Type I sites.

The origin of the enhanced $CH_3O_{(a)}$ decomposition activity at Type I sites can be attributed to the higher basicity of the lattice O^{2-} anion at the cation vacancy site. In contrast, the subsequent $HCOO_{(a)}$ decomposition step is not similarly accelerated, because the Type I lattice anion is already participating in the $HCOO_{(a)}$ group itself:

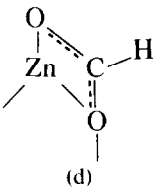

The fact that the Type I sites were still blocked after the $CH_3O_{(a)}$ to $HCOO_{(a)}$ conversion step indicates that the $HCOO_{(a)}$ species does involve the Type I O^{2-} anion, as suggested in structure (d). The fact that formate species adsorbed in Type I sites decompose to yield CO instead of CO_2 may be attributed to the difficulty of removing a threefold coordinated O^{2-} anion from the ZnO surface. At this point it is worth stressing again that the Type I sites are *not* associated with anion vacancies or electronic defects on any surface. Experiments using various pretreatments in O_2 or H_2 showed that oxidizing or reducing treatments do not significantly change the concentration of Type I sites on ZnO (*25*). Additional evidence against any significant role for O^{2-} vacancies during CH_3OH adsorption or decomposition on ZnO is provided by the absence of CH_4 as a decomposition product in these experiments. In separate experiments using a ZnO single crystal pretreated to much higher temperatures (ca. 1000 K), we showed that CH_4 evolution does occur from prism surfaces

of ZnO, but only after exposing the crystal to extreme reducing conditions (*16*). Methane evolution from these surfaces has also been reported by Kung's group (*36, 37*). Also, neither Kung's group nor our own have observed CH_4 evolution from (0001)-Zn surfaces. Thus, we conclude that O^{2-} vacancies on ZnO will only play a significant role in catalytic reactions at temperatures well above 673 K, and then only on the prism plane surfaces.

Implications for the methanol synthesis mechanism. The results described above have provided a detailed and internally consistent microscopic model for the geometry and reaction kinetics of the Type I H_2 sites. Ironically, this hard-won understanding now leads us to seriously question the importance of these Type I sites as active sites for the methanol synthesis reaction in Cu/ZnO catalysts. In no case did we observe CH_3OH desorption from $CH_3O_{(a)}$ species adsorbed in Type I sites. We did observe a well defined desorption process for H_2O, but with a desorption energy of 40 kcal/mol, significantly higher than for the majority of the dissociatively adsorbed H_2O states. We propose that this strong H_2O adsorption energy reflects the basicity of the Type I lattice O^{2-} anion. This also suggests that recombinative CH_3OH desorption step would also be more difficult from Type I sites, relative to other sites on the ZnO surface.

We did observe a modest enhancement for the $CH_3O_{(a)}$ decomposition step at Type I sites. However, it does not necessarily follow that the activation energy for the reverse reaction (i.e., $CH_3O_{(a)}$ formation from $HCOO_{(a)}$) is also reduced. Moreover, we have recently studied the kinetics of CH_3OH decomposition on evaporated Cu/ZnO thin films (*12*). This permitted us to measure the reaction kinetics simultaneously on both the Cu and ZnO components of the same sample. The enhancement observed for both the $CH_3O_{(a)}$ and $HCOO_{(a)}$ decomposition steps on Cu relative to ZnO was much larger than the enhancement seen here for $CH_3O_{(a)}$ decomposition at Type I vs non-Type I sites. This suggests that the presence of the Cu component will have a more important influence than the presence of geometrically distinct Type I sites.

Finally, the large binding energy observed for H_2O in Type I sites suggests that these sites may be blocked under synthesis conditions, since the reactant mixture used in commercial processes usually includes a small amount of added CO_2 that would be converted to H_2O via the reverse shift reaction.

Thus the present results strongly suggest that the origin of the methanol synthesis activity in the Cu/ZnO catalyst system does not reside in the Type I sites found on ZnO. This suggests that efforts to develop improved CH_3OH synthesis catalysts should not be aimed at attempting to increase and/or stabilize the concentration of Type I sites.

These results do not rule out the possibility that analogous sites may be present at isolated Cu cations on the surface of Cu/ZnO catalysts (*13*). Experiments similar to those described here for pure ZnO are presently underway in our laboratory to identify the adsorption sites and decomposition kinetics for CH_3OH on various Cu/ZnO mixtures.

ACKNOWLEDGMENTS

This work was partially supported by the National Science Foundation, Grant NSF-RIG-CPE 8105823. One of us (D. L. R.) acknowledges stipend support from Chevron Research Company, Standard Oil of California.

REFERENCES

1. Herman, R. G., Klier, K., Simmons, G. W., Finn, B. P., Bulko, J. B., and Koblyinski, T. P., *J. Catal.* **56,** 407 (1979).
2. Mehta, S., Simmons, G. W., Klier, K., and Herman, R. G., *J. Catal.* **57,** 339 (1979).
3. Klier, K., Chatakavanij, V., Herman, R. G., and Simmons, G. W., *J. Catal.* **74,** 343 (1982).
4. Klier, K., "Advances in Catalysis," Vol. 31, p. 243. Academic Press, New York, 1982.
5. Bowker, M., *Vacuum* **33,** 669 (1983).
6. Edwards, J. F., and Schrader, G. L., *J. Catal.* **94,** 175 (1985).

7. Chinchen, G. C., Denny, P. J., Parker, D. G., Short, G. D., Spencer, M. S., Waugh, K. C., and Whan, D. A., *Prepr. Pap. Amer. Chem. Soc. Div. Fuel Chem.* National Meeting, Fall, 1984.
8. Andrew, S. P. S., *in* "Proceedings, 7th International Congress on Catalysis, Osaka, 1980." Post. Congr. Symp., Paper 12. Elsevier, Amsterdam, 1981.
9. Marsden, W. L., Wainwright, M. S., and Friedrich, J. B., *Ind. Eng. Chem. Prod. Res. Dev.* **19,** 551 (1980).
10. Friedrich, J. B., Wainwright, M. S., and Young, D. J., *J. Catal.* **80,** 1 (1983).
11. Friedrich, J. B., Young, D. J., and Wainwright, M. S., *J. Catal.* **80,** 14 (1983).
12. Chan, L., and Griffin, G. L., *Surf. Sci.*, in press.
13. Roberts, D. L., and Griffin, G. L., *Appl. Surf. Sci.* **19,** 298 (1984).
14. Griffin, G. L., and Yates, J. T., Jr., *J. Chem. Phys.* **77,** 3744 (1982).
15. Griffin, G. L., and Yates, J. T., Jr., *J. Chem. Phys.* **77,** 3751 (1982).
16. Chan, L., and Griffin, G. L., *Surf. Sci.* **155,** 400 (1985).
17. Edwards, J. F., and Schrader, G. L., *J. Phys. Chem.* **89,** 782 (1985).
18. Boccuzzi, F., Garrone, E., Zecchina, A., Bossi, A., and Camia, M., *J. Catal.* **51,** 160 (1978).
19. Bowker, M., Houghton, H., Waugh, K. C., Giddings, T., and Green, M., *J. Catal.* **84,** 252 (1983).
20. Grunze, M., Hirschwald, W., and Hofmann, D., *J. Cryst. Growth* **52,** 241 (1981).
21. Lavalley, J. C., Saussey, J., and Rais, T., *J. Mol. Catal.* **17,** 289 (1982).
22. Saussey, J., Lavalley, J. C., Lamotte, J., and Rais, T., *J. Chem. Soc. Chem. Commun.*, 278 (1982).
23. Saussey, J., Lavalley, J. C., Rais, T., Chakor-Alami, A., Hindermann, J. P., and Kiennemann, A., *J. Mol. Catal.* **26,** 159 (1984).
24. Eischens, R. P., Pliskin, W. A., and Low, M. J. D., *J. Catal.* **1,** 180 (1962).
25. Dent, A. L., and Kokes, R. J., *J. Phys. Chem.* **73,** 3772 (1969).
26. Dent, A. L., and Kokes, R. J., *J. Phys. Chem.* **73,** 3781 (1969).
27. Baranski, A., and Cvetanovic, R. J., *J. Phys. Chem.* **75,** 208 (1971).
28. Baranski, A., and Galuszka, J., *J. Catal.* **44,** 259 (1976).
29. Boccuzzi, F., Borello, E., and Zecchina, A., Bossi, A., and Camia, M., *J. Catal.* **51,** 150 (1978).
30. Saussey, J., Lavalley, J. C., and Bovet, C., *J. Chem. Soc., Faraday Trans.* **1, 78,** 1457 (1982).
31. Knozinger, H., "Advances in Catalysis," Vol. 25, p. 184. Academic Press, New York, 1976.
32. Roberts, D. L., and Griffin, G. L., *J. Catal.* **93,** 400 (1985).
33. Atherton, K., Newbold, G., and Hockey, J. A., *Discuss. Faraday Soc.* **52,** 33 (1971).
34. Jones, D. M., and Griffin, G. L., *J. Catal.* **80,** 40 (1983).
35. Ueno, A., Onishi, T., and Tamaru, K., *Trans. Faraday Soc.* **67,** 3585 (1971).
36. Chen, W. H., Akhter, S., and Kung, H. H., *J. Catal.* **82,** 341 (1983).
37. Akhter, S., Chen, W. H., Lui, K., and Kung, H. H., *J. Catal.* **85,** 437 (1984).